

Chapter 10

Fourier Transform and Linear Prediction Methods

Jens J. Led and Henrik Gesmar

Chemistry Department, University of Copenhagen, Universitetsparken 5, DK-2100, København Ø, Denmark

10.1 Introduction	131
10.2 The Fourier Transform of the Free Induction Decay	132
10.3 The Linear Prediction Method	134
10.4 Least-Squares Fourier Transform Techniques	139
10.5 Conclusion	141
References	141

10.1 INTRODUCTION

In the CW NMR technique, as used in the early days of NMR, the frequency spectrum was obtained directly as a function of the input rf or the strength of the magnetic field, B_0 . For the modern high resolution pulse NMR experiment a FID is recorded as a function of time, and the frequency spectrum is calculated as the FT of this time domain signal. Despite the qualities of the FT, such as computational efficiency and numerical stability, in recent years improved spectral methods have been introduced into the analysis of NMR data. Among these methods the linear prediction method, described in this chapter, has been one of the most successful.

There are two main reasons for the application of the linear prediction method to NMR data. One is to produce better spectra, i.e. to avoid the drawbacks that characterize the FT, particularly for multidimensional NMR data (see Chapters 1 and 2). The other reason for the use of the linear prediction method is to estimate spectral parameters (frequencies, signal intensities, signal widths, and phases) directly from the FIDs.

The drawbacks of the FT mentioned above are aliasing, $(\sin x)/x$ convolution of the resonance signals, phase distortions, and pseudobaselines. Although we often refer to these effects as artifacts, they are caused by one of the advantages of the FT, i.e. the conservation of information. Thus, the fact that the time domain FID can be sampled only for a finite period of time and only as a limited number of discrete data points, must also be expressed in the frequency spectrum. Unfortunately, this information is kept in the form of the rather annoying effects mentioned above. These characteristics of the FT are quite general. In 10.2 of this article they are described in some detail for the special case of the NMR FID.

From the above it follows that in order to reduce the ‘artifacts’ in the spectrum we must apply an alternative spectral method that does not preserve all the information of the FID. In particular, we wish to suppress the information about the truncation, and

preserve the information about the NMR resonance signals. As described in 10.3, this can be done by using the linear prediction method. Finally, in 10.4 it is described how a detailed knowledge of the artifacts in the FT spectrum together with the principle of least squares can be applied to gain valuable information from NMR spectra.

10.2 THE FOURIER TRANSFORM OF THE FREE INDUCTION DECAY

On the assumption of multiple exponential decays the sampled FID F_k can be expressed as

$$F_k = F(k\Delta t) = \sum_{j=1}^p I_j \exp[(i2\pi v_j - R_{2j}^*) \times (k\Delta t + T_{in}) + i\phi_j] \quad (10.1)$$

where k is an integer in the interval $[0, N-1]$, Δt is the sampling interval, I_j is the amplitude of the j th exponential, and v_j , R_{2j}^* , and ϕ_j are the frequency, the decay rate, and the phase, respectively. For severe overlap, strong coupling, or cross-correlation it may not be possible to assign I_j to a specific nucleus, but this has no consequence for the following. Further, the symbol T_{in} is the initial time during which the signal has developed before the sampling is started, and i is the imaginary unit. Equation (10.1) represents the case of quadrature detection, where the signal is sampled as a series of complex numbers. To describe the real-valued case, which is not covered in this article, equation (10.1) should be added to its own complex conjugate.

Because of the discrete nature of F_k , the FT must be applied in its discrete form, i.e.

$$S_m = S\left(\frac{m}{n\Delta t}\right) = S\left(\frac{m}{T_{aq}}\right) = \sum_{k=0}^{N-1} F_k \exp(i2\pi km/n) \quad (10.2)$$

When F_k from equation (10.1) is introduced into equation (10.2), the expression can be evaluated as the finite sum of a geometrical progression. Thus, the analytical expression for the FT NMR spectrum

is

$$S_m = S\left(\frac{m}{N\Delta t}\right) = S(\nu) = \sum_{j=1}^p A_j \frac{1 - \exp\{[i2\pi(\nu_j - \nu) - R_{2j}^*]T_{aq}\}}{1 - \exp\{[i2\pi(\nu_j - \nu) - R_{2j}^*]/F\}} \quad (10.3)$$

Here, ν_j is the independent frequency variable in the spectrum, $T_j = N\Delta t$ is the acquisition time, $F = (1/\Delta t)$ is the spectral width, and A_j is given by

$$A_j = I_j \exp[(i2\pi \nu_j - R_{2j}^*)T_{in} + i\phi_j] \quad (10.4)$$

Contrary to k , the number m is not necessarily an integer. This reflects the fact that the spectrum can be evaluated for any value of the frequency ν . However, when the fast FT procedure is applied to the N values of F_k , the spectrum is calculated only for integer values of m in the interval $[0, N-1]$. If zeros are added at the end of the FID before the FT, the right-hand side of equation (10.3) still holds, because only zeros are added to equation (10.2), but the variable m may now be a noninteger. If for example N zeros are added after the N points of the FID, the spectrum is calculated for $m=0, 1/2, 1, \frac{3}{2}, \dots, N-1$.

Equation (10.3) consists of two periodic terms: one in the numerator with the period $1/T_{aq}$, and one in the denominator with the period $F = (1/\Delta t) = (N/T_{aq})$. Thus the entire expression has a period of F , i.e. the Nyquist frequency.¹ In order to avoid the implied aliasing of signals, a sufficiently short dwell time, Δt , must be chosen in order to assure that F is larger than all resonance frequencies in the spectrum. However, as shown in equation (10.3), the discrete spectrum still differs significantly from the theoretical spectrum, which is given as a sum of nonperiodic complex Lorentzians:

$$s(\nu) = \sum_{j=1}^p \exp(i\phi_j) I_j / R_{2j}^* \frac{1}{1 - i2\pi(\nu_j - \nu)/R_{2j}^*} \quad (10.5)$$

For the discrete spectrum to approximate the theoretical spectrum, F must be large compared with the involved decay rates R_{2j}^* , and to all relevant values of $\nu_j - \nu$. The latter condition corresponds to what is often referred to as 'oversampling', and is rarely fulfilled, particularly in multidimensional spectroscopy.

Nonetheless, when these conditions hold, equation (10.3) is reduced to

$$S(\nu) = \left(F \sum_{j=1}^p \frac{A_j}{R_{2j}^*} \times \frac{1}{1 - i2\pi(\nu_j - \nu)/R_{2j}^*} + \sum_{j=1}^p A_j/2 \right) \times \{1 - \exp\{[i2\pi(\nu_j - \nu) - R_{2j}^*]T_{\text{aq}}\}\} \quad (10.6)$$

as shown by Gesmar *et al.*² If the FID is allowed to decay completely during the sampling, i.e. $T_{\text{aq}} \gg (1/R_{2j}^*)$, the term in the second parentheses in equation (10.6) is very close to unity. This is the ideal discrete FT spectrum in that it is the best approximation to a sum of complex Lorentzians as expressed in equation (10.5). Even in this case, however, the FT spectrum differs from the theoretical spectrum. Firstly, because a frequency-independent term $\sum_{j=1}^p A_j/2$ is present, and secondly, because each intensity I_j has been multiplied by the factor $\exp[(i2\pi\nu_j - R_{2j}^*)T_{\text{in}}]$, as can be seen from equation (10.4).

The first deviation results in a pseudobaseline in the FT spectrum. However, this pseudobaseline is removed in the ideal case when the first point of the FID is multiplied by $1/2$ before the Fourier transformation. This is particularly important for multidimensional spectroscopy, where the presence of baselines in the individual FIDs leads to ridges in the various dimensions.

The second deviation, namely the presence of the factor $\exp[(i2\pi\nu_j - R_{2j}^*)T_{\text{in}}]$, results in a frequency- and relaxation-dependent phase distortion of the FT spectrum. This phase distortion depends linearly upon the center frequencies ν_j of the individual signals, and not upon the independent spectral frequency variable ν . Therefore, the commonly used linear phase correction procedure, based on a linear relationship between the phase and the spectral frequency ν , is not always appropriate, although it suffices in most cases with modest phase distortions and narrow and well-separated signals. For extreme phase distortions, however, or for signals that are broad and poorly separated, or when small signals are situated on the tail of a larger signal, the spectrum can be correctly phased only at the center of each signal, and undulations of the signal tails will occur. In order to reduce such effects, the value of T_{in} is normally kept

as small as possible, despite the fact that the first few points of the FID are often of poor quality due to the electronic filtering and, occasionally, overflow in the analog-to-digital converter. Thus, not even the ideal discrete Fourier transform spectrum is the 'true' spectrum as given by equation (10.5).

In many cases, and particularly in multidimensional spectroscopy, the FID is not sampled until the point where it has decayed completely, i.e. $T_{\text{aq}} \approx 1/R_{2j}^*$. In such cases, $1 - \exp\{[i2\pi(\nu_j - \nu) - R_{2j}^*]T_{\text{aq}}\}$ in equation (10.6) cannot be neglected, which results in an apparently misphased signal. Because the phase error depends on the position of the resonance frequency ν_j relative to the specific frequencies $\nu = (m/T_{\text{aq}})$ calculated by means of the FT procedure (see above), it appears to be random and cannot be corrected in the general case. Note that for signals with $\nu_j = (m/T_{\text{aq}})$ (m is an integer), misphasing due to the truncation will not occur. Furthermore, because the pseudobaseline level $\sum_{j=1}^p A_j/2$ is also altered by $1 - \exp\{[i2\pi(\nu_j - \nu) - R_{2j}^*]T_{\text{aq}}\}$, the above-mentioned multiplication of the first data point by a factor of $1/2$ will not work, and the area between the signal curve and the baseline is no longer a measure of the relative signal intensity. The amount of intensity that has leaked into the pseudobaseline depends on ν_j and R_{2j}^* for individual resonances. As can be seen from equation (10.6), the pseudobaseline problems are reduced considerably when the spectral width F is significantly larger than the frequency range covered by the resonances, i.e. when the FID is oversampled (see above).

When m is an integer, $1 - \exp\{[i2\pi(\nu_j - \nu) - R_{2j}^*]T_{\text{aq}}\} = 1 - \exp[(i2\pi\nu_j - R_{2j}^*)T_{\text{aq}}]$ and no oscillations are observed in the spectrum. However, as already mentioned, by zero filling the FID, the frequencies $\nu = (m/T_{\text{aq}})$ in the FT spectrum can be calculated for fractional values of m also, in order to increase spectral resolution. In this case the periodicity of the factor $1 - \exp\{[i2\pi(\nu_j - \nu) - R_{2j}^*]T_{\text{aq}}\}$ is seen in the spectrum as signal side lobes ('wiggles') with a period of T_{aq}^{-1} in connection with the resonances whose components in the free induction decay have been truncated.

In the following sections it is described how the deviations between the theoretical spectrum [equation (10.5)] and the discrete FT spectrum can be reduced or even eliminated.

10.3 THE LINEAR PREDICTION METHOD

Since linear prediction was introduced into the field of NMR spectroscopy by Barkhuijsen *et al.*, it has been used as an effective tool in the analysis of time domain NMR data.^{3,4} It is applied in a number of ways, both qualitatively and quantitatively. Qualitatively it is used as a preprocessor to the FT in order to improve the resulting spectra. Quantitatively it can be used as an estimator of the spectral parameters, i.e. the frequencies, linewidths, intensities, and phases. In all cases, it eliminates or reduces considerably the deficiencies of the FT such as aliasing, truncation errors, phase distortions, and ridges in one- and multi-dimensional NMR spectra. In this section the principles of the linear prediction method are reviewed briefly. In 10.3.1 the qualitative application of the method is illustrated, and the quantitative application of the linear prediction method is demonstrated in 10.3.2.

The FID signal F_k , given as a sum of p exponentially damped sinusoids sampled at regular time intervals [equation (10.1)], has the following property:

$$F_k = \sum_{m=1}^p f_m F_{k-m} \quad (10.7)$$

disregarding the effect of the noise.⁵ Here f_m is the m th forward prediction coefficient. Since f_m is independent of k it can be determined from the experimental data points, and subsequently used to extrapolate the FIDs. An interesting alternative to direct extrapolation of the FID, the linear prediction z -transformation (LPZ) method, has been suggested by Tang and Norris.⁶

The prediction coefficients are related to the frequencies ν_j and the decay rates R_{2j}^* , through the characteristic polynomial:

$$z^p - \sum_{m=1}^p f_m z^{p-m} = P(z) \quad (10.8)$$

since the roots C_j of this polynomial are given by⁵

$$C_j = \exp[(i2\pi\nu_j - R_{2j}^*)\Delta t] \quad (10.9)$$

For an experimental FID, the precise number of signals contained in the FID is, in general, unknown a priori. Therefore, the applied number of prediction coefficients must be sufficiently large ($>p$) to ensure

the determination of all the involved complex exponentials. This results in an excess of roots of the characteristic polynomial in equation (10.8). However, as shown by Kumaresan,⁷ the roots are divided into two classes: one that contains the p signal roots conforming to equation (10.9), and another that contains the extraneous roots. Furthermore, in the case of backward prediction, i.e.

$$F_k = \sum_{m=1}^p b_m F_{k+m} \quad (10.10)$$

the two classes can be separated, since the extraneous roots still fall inside the unit circle, whereas the signal roots C_j are situated outside the unit circle. In the case of forward prediction [equation (10.7)], both classes fall inside the unit circle. This is, in principle, of no consequence if the coefficients are used for an extrapolation of the FID, since this requires both classes of coefficient. In practice, however, the presence of noise may occasionally result in roots that fall outside the unit circle, corresponding to noise components with negative decay rates (see below).

10.3.1 Qualitative Application

Qualitatively, linear prediction is used as a preprocessor to the FT in order to improve the resulting spectra.⁴ An example of this application is the reconstruction of the first few data points of an experimental FID where these points have been corrupted by pulse breakthrough or by electronic filtering.⁸ The presence of such corrupted data points may result in a severe baseline distortion, as illustrated in Figures 10.1(a) and (b). Although a deletion of the points would, in principle, remedy this problem, such a deletion would create a new problem, namely a dramatic first-order phase distortion of the FT spectrum. However, as shown in Figures 10.1(c) and (d), a reconstruction of the first six data points from the succeeding ones using equation (10.10) results in a straight baseline of the FT spectrum. Obviously, backward linear prediction extrapolation of the FID also provides a method of correcting dramatic first-order phase distortions, as occurs in cases where the experimental conditions introduce significant initial delays, e.g. semiselective soft pulses.

For truncated FIDs, forward extrapolation can be applied in order to reduce the truncation errors, and thus increase the resolution.⁹ This is particularly

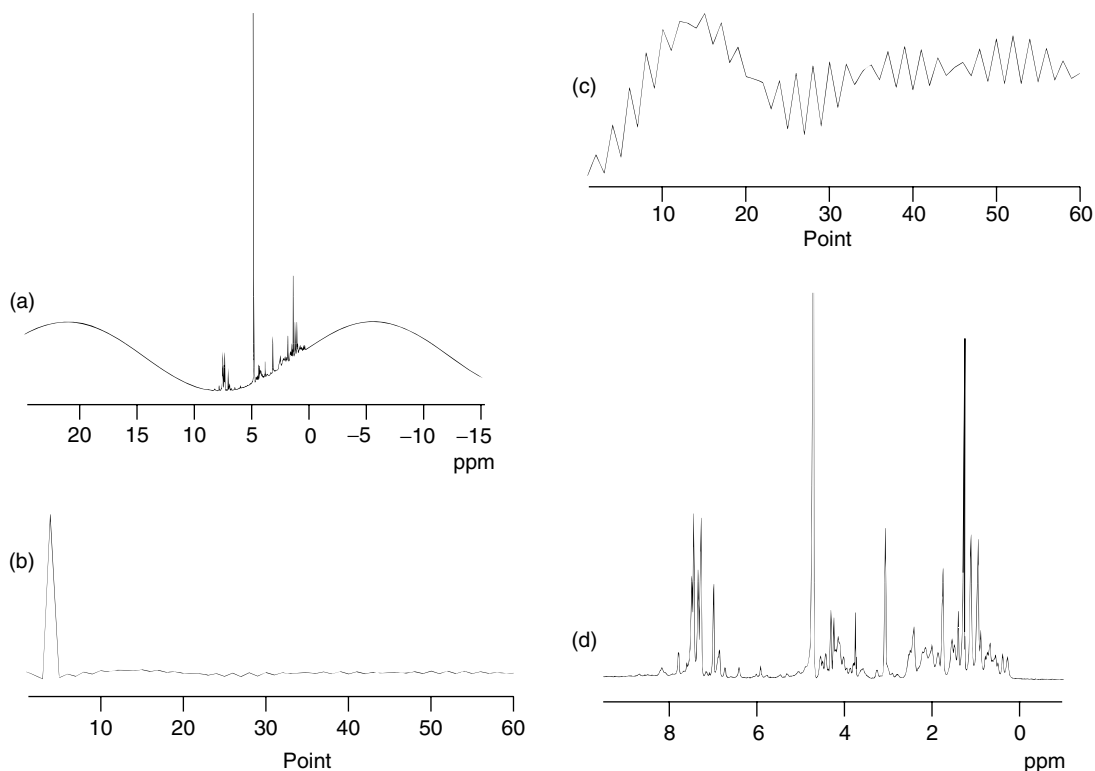


Figure 10.1. The first slice ($t_1 = 0$) along the second dimension in a two-dimensional ^1H HOHAHA dataset for dimeric insulin. (a) The FT spectrum. (b) The first 50 data points of the FID. Note that the fourth data point in the FID is severely damaged, which gives rise to the undulating baseline in (a). (c) The first six data points of the FID were deleted and recalculated from 18 linear prediction coefficients using equation (10.10). The linear prediction coefficients were determined from 36 equations of the type of equation (10.10), k ranging from 7 to 42. Note that the vertical scale is changed. (d) The FT spectrum of the repaired FID. Note that both scales are changed. (Reproduced by permission of The American Chemical Society from J. J. Led and H. Gesmar, *Chem. Rev.*, 1991, **91**, 1413.)

the case in three- or higher-dimensional spectra.^{10,11} Because of a limited accumulation time, the time domain data for the slowest incrementing time dimension are normally truncated, which results in a limited resolution. Also, for natural abundance two-dimensional heteronuclear correlation spectra, forward extrapolation has proved useful. Because of the low sensitivity that characterizes these spectra, the data acquisition in the t_1 domain should be confined to only the first and most intense part of the FID. This, however, is meaningful only if the associated truncation errors can be alleviated by forward linear prediction of the FID.

In both cases of forward extrapolation the reliability of the extrapolation depends on the number and the quality of the experimental data used for the

extrapolation. This can be realized by considering a noiseless FID containing N sinusoids. Here only $4N$ data points would be necessary to determine the $4N$ parameters that are involved (i.e. the frequencies, the linewidths, the intensities, and the phases of the N signals) and, thereby, to reproduce the entire FID. When noise is present, as in experimental data, the number of data points and linear prediction coefficients used for the extrapolation must be increased considerably. Normally, the number of data points should exceed the number of linear prediction coefficients by at least a factor of 3.

As mentioned above, the noise may also give rise to roots outside the unit circle. Since these roots correspond to noise components with negative decay rates, an extrapolation that includes the

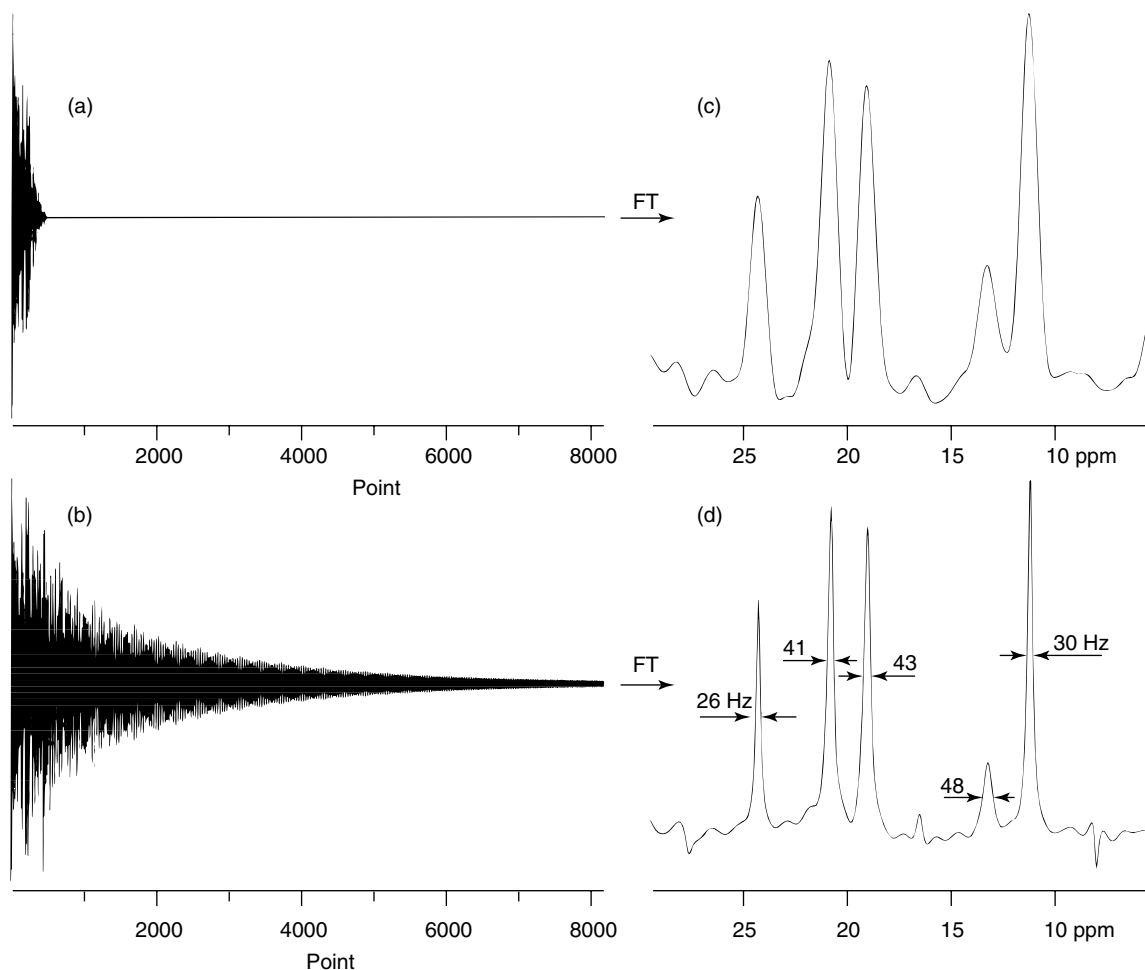


Figure 10.2. An experimental FID along t_1 (512 data points, t_1 acquisition time 10.2 ms) in a heteronuclear multiple quantum coherence C–H correlated two-dimensional spectrum of insulin. (a) Zero filled to 8192 data points and digital-filtered using a \cos^2 window function. (b) Linear prediction extrapolated to 8192 data points using equation (10.7). (c) FT of the digital-filtered FID in (a). (d) FT of the linear prediction extrapolated FID in (c). (Reproduced by permission of ESCOM Science Publishers B.V. from J. J. Led and H. Gesmar, *J. Biomol. NMR*, 1991, **1**, 237.)

corresponding linear prediction coefficients would result in an extrapolated FID which increases with increasing time. Preferably, this problem should be solved by including more experimental information in order to obtain a more stable solution, and thus remove the extracircular roots and ensure the decay of the extrapolated FID. If this is not possible, the roots may simply be reflected to fall inside the unit circle.⁸ In any case, it is mandatory to apply equation (10.10) in order to check for roots outside the unit circle and, if necessary, to construct a modified set of roots from

which a new set of linear prediction coefficients can be calculated. Omission of this procedure may result in artifactual peaks in the resulting spectra.

The effect of forward extrapolation is illustrated in Figure 10.2 which shows an experimental FID along the t_1 dimension in the methyl region of the C–H correlation spectrum of insulin, together with the FT. The original time domain data were Fourier transformed in t_2 , so that the FID in Figure 10.2 is a sum of several proton signals modulated by the frequencies of the attached ^{13}C nuclei. Here Fourier

transformation of the original 512 experimental data points alone would result in an unacceptably low digital resolution, while zero filling would give rise to truncation errors in the form of a sinc function ('wiggles') superimposed on the signals. Although this artifact can be removed by digital filtering [Figures 10.2(a) and (c)], it can be done only by sacrifice of resolution. Only if the FID is extrapolated by linear prediction to an almost complete decay [Figure 10.2(b)] is the information, inherent in the experimental FID, retained [see Figure 10.2(d)].

It should be emphasized that, whereas the backward reconstruction of the first few corrupted data points of the FID is normally a 'safe' modification, the forward extrapolation of a FID should be applied with care. This holds because the number of reconstructed data points in the backward reconstruction is small compared with the number of linear prediction coefficients that can be calculated, and because the fine structure of the spectrum is not influenced by the initial points in the FID. Similar favorable conditions do not apply in the case of forward prediction, since here a more extensive extrapolation is often desirable in order to ensure a complete decay. In general, the number of complex linear prediction coefficients must be at least equal to the number of resonances in the FID, and preferably exceed it by several factors, the surplus necessary depending on the signal-to-noise ratio. Should this condition not be fulfilled, the accuracy by which the frequencies are reproduced by the extrapolation may be too low, making the extrapolation less valuable, or even meaningless, if carried too far. In such cases a shorter extrapolation in combination with a window function may be appropriate.¹⁰

10.3.2 Quantitative Applications

10.3.2.1 One-Dimensional Data

The aim of the quantitative linear prediction approach is to obtain the spectral information from the FID directly as the parameters I_j , ν_j , R_{2j}^* , and ϕ_j , i.e. to estimate the involved intensities, frequencies, decay rates, and phases. In addition, the corresponding standard deviations should be evaluated. The quantitative linear prediction method is based on the classical work by Baron de Prony, further developed by Kumaresan and Tufts, and introduced into the field of

NMR spectroscopy by Barkhuijsen *et al.* as the linear prediction singular value decomposition method (LPSVD).^{3,12,13} The basic principle of the method is described below.

In order to find n linear prediction coefficients from N data points, equation (10.10) is set up for $N - n$ values of the index k , where n should be chosen to be considerably larger than the expected number of resonances. The linear prediction coefficients are found by singular value decomposition of equation (10.10), and subsequently the roots of the characteristic polynomial in equation (10.8) are found. As explained in the previous section, the extraneous roots, caused by the excess of linear prediction coefficients, can be separated from the signal roots C_j because the former fall inside the unit circle, while the latter fall outside because of the decay of the complex exponentials. For backward prediction $C_j = \exp [(-i2\pi\nu_j + R_{2j}^*)\Delta t]$ and F_k can be expressed as

$$F_k = F(k \Delta t) = \sum_{j=1}^p I_j \exp(i\phi) C_j^{-(k+T_{in}/\Delta t)} \quad (10.11)$$

where F_k is seen to depend linearly on $I_j \exp(i\phi)$. For N data points, equation (10.11) can be expressed for N values of k , and because $C_j^{-(k+T_{in}/\Delta t)}$ is known, the complex values of $I_j \exp(i\phi)$ can be determined by a linear least-squares calculation. From the complex values of C_j and $I_j \exp(i\phi)$, the spectral parameters ν_j , R_{2j}^* , I_j , and ϕ_j are easily determined. Thus, the spectral parameters needed to describe the resonances in the FID can be determined without any a priori assumptions about their values. As only the parameters I_j and ϕ_j are included in the final least-squares calculation, true least-squares estimates of the standard deviations cannot be evaluated from the corresponding normal equation matrix. However, as established by Barkhuijsen *et al.*¹⁴ in a later paper, the Cramér Rao lower bounds can be used as reasonable substitutes.

Although the spectral parameters contain all the relevant information about the FID, a noiseless FID is often simulated and subsequently Fourier transformed to make a direct comparison with the FT spectrum possible. An example from the original paper by Barkhuijsen *et al.*³ is shown in Figure 10.3.

The fact that no initial assumption about the spectral parameters is needed increases the value of the linear prediction method for complicated spectra with many narrowly spaced and overlapping

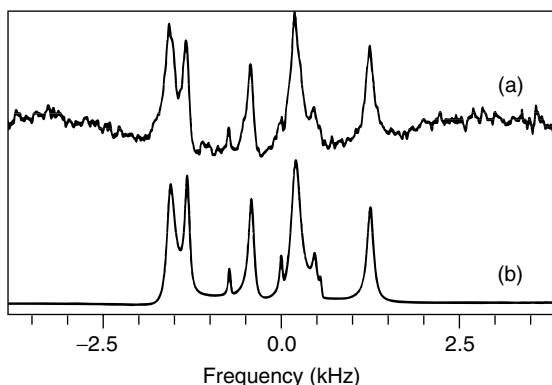


Figure 10.3. (a) In vivo ^{31}P NMR spectrum, computed by cosine fast Fourier transformation of 768 data points, using the optimal signal-to-noise ratio filter with a time constant of 0.015 s, and putting the three initial data points equal to zero. (b) Graphical display of the linear prediction singular value decomposition results, extracted from data points 4 to 128. This was obtained by cosine fast Fourier transformation of 768 data points computed from the estimated parameters. (Reproduced by permission of Academic Press, Inc. from H. Barkhuijsen, R. de Beer, W. M. M. J. Bovée, and D. van Ormondt, *J. Magn. Reson.*, 1985, **61**, 465.)

resonances. In order to ensure sufficient resolution in such cases a very large number of linear prediction coefficients is needed in equation (10.10). This often results in computations that are unfeasible with the classical procedures for solving linear equations such as singular value decomposition, QR, and Cholesky decomposition, all of which have been applied to the linear prediction method in order to solve equation (10.10).^{15,16} Therefore, dedicated fast algorithms have been developed for both the singular value decomposition method and the QR method.^{17,18} Consequently, for one-dimensional linear prediction calculations the computational bottleneck is no longer associated with solving equation (10.10), but rather with the rooting of the characteristic polynomial. As shown in Figure 10.4, it is possible, at present, to apply more than 10 000 linear prediction coefficients to ensure sufficient resolution.

10.3.2.2 Two-Dimensional Data

The complete quantitative linear prediction analysis of two-dimensional NMR data was developed by Gesmar and Led, as reviewed briefly here.¹⁹ A two-dimensional FID, $F_{l,k} = F(l\Delta t', k\Delta t)$, sampled

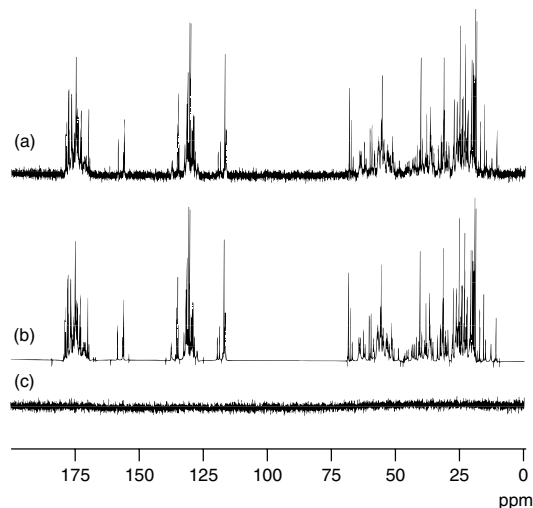


Figure 10.4. (a) FT ^{13}C spectrum of the dimeric insulin. The corresponding FID was recorded at 305 K and 125.76 MHz in 32 k data points with a sweep width of 50 000 Hz. (b) The FT of the FID recalculated from the spectral parameters produced by a 13 000 order fast linear prediction calculation on the experimental FID. (c) The difference between the FT spectrum in (a) and the fast linear prediction spectrum in (b). (Reproduced by permission of Academic Press, Inc. from H. Gesmar and P. C. Hansen, *J. Magn. Reson.*, 1994, **106**, 236.)

at regularly spaced time intervals Δt and $\Delta t'$ in the two dimensions, conforms with equation (10.1) only if $I_j \exp(i\phi_j)$ is substituted by

$$D_{l,j} = \sum_{h=1}^{p_j} I_{h,j} \exp(i\phi_{h,j}) \exp[(i2\pi\nu'_h - R_{2h}^*)l\Delta t'] \quad (10.12)$$

where the label prime indicates the second dimension. The parameter $I_{h,j}$ is the intensity of the two-dimensional signal and p_j is the number of correlations of the j th resonance. Equation (10.10) is still valid for any value of l , and because $\exp[(i2\pi\nu_j - R_{2j}^*)\Delta t]$ does not depend on l , neither do the backward coefficients b_m . Thus, an equation similar to equation (10.10)

$$F_{l,k} = \sum_{m=1}^p b_m F_{l,k+m} \quad (10.13)$$

applies in the two-dimensional case for any value of k and l , i.e. the p linear prediction coefficients apply in

the t dimension for all values of l . Therefore, equation (10.13) can be set up and solved for all values of l simultaneously. After the determination of the b_m values, the corresponding characteristic polynomial equation is solved, and the frequencies ν_j and the decay rates R_{2j}^* are found from the C_j values for the t dimension exactly as in the one-dimensional case. Since the C_j values are known at this point, the values of the $D_{l,j}$ terms that have replaced the I_j terms can be found for each value of l in the same way as the I_j values were found for the one-dimensional case. Thus, for each resonance ν_j a series of values of $D_{l,j}$ as a function of l can be evaluated. Now, because $D_{l,j}$ itself is a sum of complex exponentials, as can be seen from equation (10.12), the linear prediction principle applies once again. Therefore,

$$D_{l,j} = \sum_{m=1}^{p_j} b'_{j,m} D_{l+m,j} \quad (10.14)$$

where $b'_{j,m}$ represents the t' backward coefficients that belong to the j th resonance. For each resonance ν_j a complete one-dimensional linear prediction calculation, which also includes the rooting of the characteristic polynomial and subsequent linear least-squares determination of the intensities and phases, is carried out. Thus, in addition to ν_j and R_{2j}^* , estimates of ν_{hj}' and R'_{2hj}^* are produced together with the value of I_{hj} and ϕ_{hj} , i.e. a complete determination of the spectral parameters of the two-dimensional FID has been achieved.

The applicability of the two-dimensional quantitative linear prediction procedure was demonstrated in the original paper by the determination of the spectral parameters from the ^1H phase modulated COSY FID of threonine in D_2O .¹⁹ The parameters are listed in the original paper, and the quality of the estimation is illustrated in Figure 10.5 by a two-dimensional Lorentzian-shaped reconstruction of a $(\beta\text{-CH}, \text{CH}_3)$ cross peak.

10.4 LEAST-SQUARES FOURIER TRANSFORM TECHNIQUES

In this section it is described how the spectral parameters I_j , ν_j , R_{2j}^* , and ϕ_j can be estimated from the FT spectrum, unbiased by the deviations from the theoretical spectrum described in 10.2.²⁰ As mentioned previously, no information is lost by the Fourier transformation and, therefore, the spectral parameters can

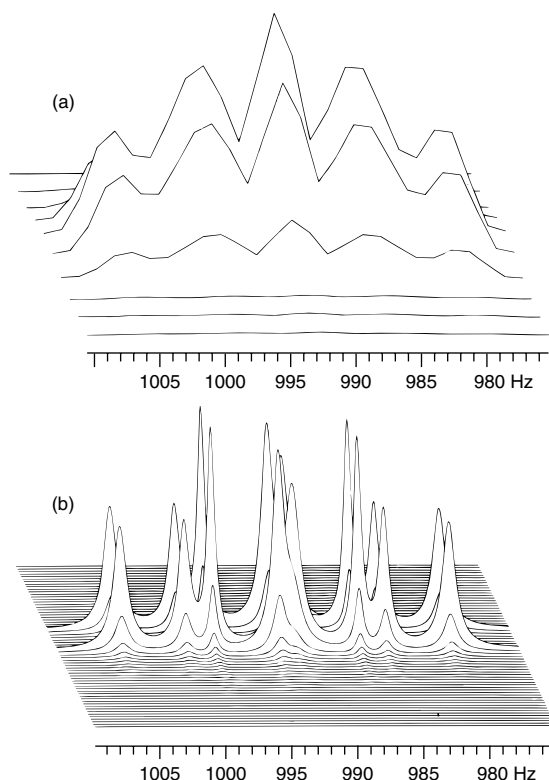


Figure 10.5. (a) Expansion of the $(\beta\text{-CH}, \text{CH}_3)$ multiplet in the sine bell filtered two-dimensional absolute mode Fourier transform spectrum. (b) Spectrum of the same region, calculated from the parameters estimated by the two-dimensional linear prediction procedure. The signals are pairwise in counterphase, but the phases have been set to zero in the displayed spectrum. (Reproduced by permission of Academic Press, Inc. from H. Gesmar and J. J. Led, *J. Magn. Reson.*, 1989, **83**, 53.)

be evaluated from the FT spectrum as well as from the FID. Furthermore, the noise in the FT spectrum is uncorrelated with the zero mean and constant variance if the same holds for the FID, a condition that is generally assumed to be true.² Thus the spectral parameters I_j , ν_j , R_{2j}^* , and ϕ_j can be estimated by a nonlinear least-squares fit of equation (10.3) to the FT spectrum. It should be emphasized, however, that unbiased estimates of the spectral parameters are obtained only by application of this exact expression for the discrete FT of a multiexponential decaying FID. Any attempt to fit Lorentzian signals to the FT spectrum will lead to biased values of the spectral parameters, as discussed in 10.2. In order to ensure that

the spectral noise is uncorrelated, it is also important that the FID is neither zero filled nor manipulated in any other way.

An example that demonstrates the result of a least-squares fit of equation (10.3) to an FT spectrum is shown in Figure 10.6. Here the ^1H FT NMR spectrum of *N*-methylacetamide in water is presented together with a simulated spectrum, recalculated from the parameters estimated in the least-squares fit. The small signals are ^{13}C satellites from the abundant *trans* isomer and the methyl resonances from the *cis* isomer. Because of the 6000 : 1 intensity ratio between the large water signal and the smallest signals of the solute, the latter are severely affected by aliasing. However, because equation (10.3) is used in the least-squares analysis, unbiased spectral parameters are obtained for all signals, even the small ones. Thus, the intensity ratio between the methyl signals of the *trans* isomer and their ^{13}C satellites was estimated as $1.11\% \pm 0.10\%$, which is in agreement with the expected concentration ratio of 1.12%. Likewise, the concentration of the *cis* isomer at 300 K was estimated to $1.60\% \pm 0.10\%$ of the total amount of *N*-methylacetamide. This also compares favorably with the previously estimated value of 3%. A table, that contains all the estimated spectral parameters and their standard deviations can be found in the original paper.²⁰

Because the spectrum $S(\nu)$ represented by equation (10.3) depends on the resonance frequency ν_j and the decay rate R_{2j}^* in a nonlinear fashion, the least-squares analysis must be performed iteratively and requires an estimate of reasonable initial values of these nonlinear parameters. This represents a difficult and time-consuming task and may even be impossible for complicated spectra. One way to solve this problem is to perform a linear prediction analysis of the corresponding FID and use the linear prediction estimate of the frequencies and decay rates as initial values for the least-squares iterations. Alternatively, one can proceed as proposed by Kumaresan *et al.*,²¹ who have designed a sequence of iterations that requires only very crude initial values. The advantage of this approach is that no polynomial rooting is needed, as in the linear prediction procedure. However, unlike the linear prediction procedure, no 'fast' algorithm exists for the solution of the involved equations, and thus the choice of procedure must depend on the complexity of the NMR spectrum, and on the available computational possibilities. Still, unbiased

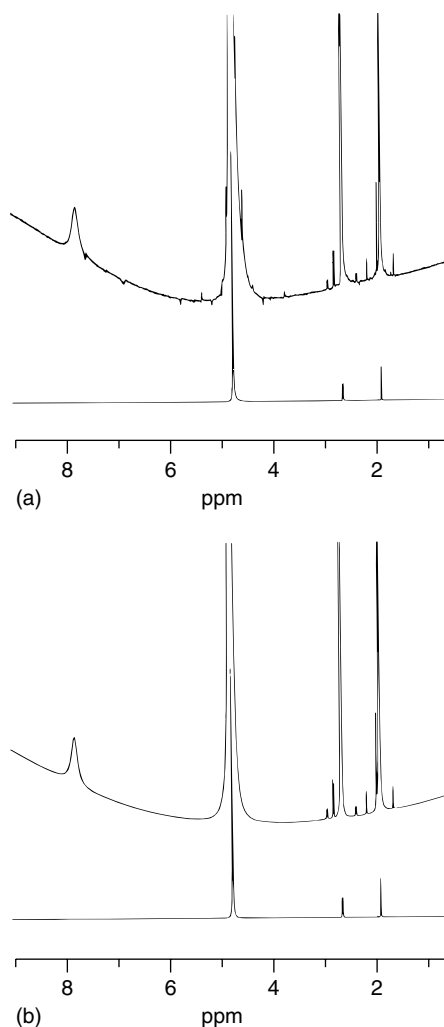


Figure 10.6. (a) The ^1H NMR absorption mode FT spectrum of a 2.5 M solution of *N*-methylacetamide in water at pH 5.2. In the upper spectrum the vertical scale is increased by a factor of 100. (b) Simulated spectrum based on the parameters derived from the experimental spectrum corresponding to (a). The same linear phase correction was used in both spectra. (Reproduced by permission of Academic Press, Inc. from F. Abildgaard, H. Gesmar, and J. J. Led, *J. Magn. Reson.*, 1988, **79**, 78.)

estimates of the spectral parameters I_j , ν_j , R_{2j}^* , and ϕ_j can be obtained with both methods, because both include a least-squares calculation based on equation (10.3).

10.5 CONCLUSION

The spectral methods described in this article (extrapolation of the FID by linear prediction, quantitative linear prediction, and least-squares FT) have all proved to be very useful in NMR spectroscopy. The major drawbacks of these methods have been the extensive computing time required and the need for very large amounts of computer memory. However, the new 'fast' algorithms together with the substantial improvements in minicomputers have reduced these drawbacks considerably, and made the use of linear prediction and least-squares analyses feasible on standard computational equipment that is normally available in NMR laboratories today.

RELATED ARTICLES IN THE ENCYCLOPEDIA OF MAGNETIC RESONANCE

Fourier Transform Spectroscopy The Development of NMR

REFERENCES

1. E. O. Brigham, *The Fast Fourier Transform*, Prentice-Hall, Englewood Cliffs, NJ, 1974, p. 85.
2. H. Gesmar, J. J. Led, and F. Abildgaard, *Prog. NMR Spectrosc.*, 1990, **22**, 255.
3. H. Barkhuijsen, R. de Beer, W. M. M. J. Bovée, and D. van Ormondt, *J. Magn. Reson.*, 1985, **61**, 465.
4. J. J. Led and H. Gesmar, *Chem. Rev.*, 1991, **91**, 1413.
5. S. M. Kay and S. L. Marple, Jr., *Proc. IEEE*, 1981, **69**, 1380.
6. J. Tang and R. Norris, *J. Magn. Reson.*, 1986, **69**, 180.
7. R. Kumaresan *IEEE Trans. ASSP*, 1983, **31**, 217.
8. D. Marion and A. Bax, *J. Magn. Reson.*, 1989, **83**, 205.
9. C. F. Tirendi and J. F. Martin, *J. Magn. Reson.*, 1989, **81**, 577.
10. E. T. Olejniczak and H. L. Eaton, *J. Magn. Reson.*, 1990, **87**, 628.
11. G. Zhu and A. Bax, *J. Magn. Reson.*, 1990, **90**, 405.
12. G. R. B. Prony, *J. L'École Polytech. Paris*, 1795, **1**, 24.
13. R. Kumaresan and D. W. Tufts *IEEE Trans. ASSP*, 1982, **30**, 833.
14. H. Barkhuijsen, R. van de Beer, and D. van Ormondt, *J. Magn. Reson.*, 1986, **67**, 371.
15. H. Gesmar and J. J. Led, *J. Magn. Reson.*, 1988, **76**, 183.
16. J. Tang, C. P. Lin, M. K. Bowman, and J. R. Norris, *J. Magn. Reson.*, 1985, **62**, 167.
17. W. W. F. Pijnappel, A. van den Boogaart, R. de Beer, and D. van Ormondt, *J. Magn. Reson.*, 1992, **97**, 122.
18. H. Gesmar and P. C. Hansen, *J. Magn. Reson.*, 1994, **106**, 236.
19. H. Gesmar and J. J. Led, *J. Magn. Reson.*, 1989, **83**, 53.
20. F. Abildgaard, H. Gesmar, and J. J. Led, *J. Magn. Reson.*, 1988, **79**, 78.
21. R. Kumaresan, C. S. Ramalingam, and D. van Ormondt, *J. Magn. Reson.*, 1990, **89**, 562.